Production and decay of the d^* dibaryon

Chun Wa Wong

Department of Physics and Astronomy, University of California, Los Angeles, California 90095-1547
(Received 14 October 1997)

The production of the isoscalar $J^{\pi} = 3^+$ didelta dibaryon d^* by proton inelastic scattering from deuteron targets is described in a double-scattering Glauber approximation. Each scattering changes a target nucleon into a Δ with the help of the isovector tensor force transmitted by π and ρ mesons. The differential cross section constructed from empirical Love-Franey nucleon-nucleon t matrices and a simple model of d^* shows a maximum of some 10 μb/sr at 70° (c.m.) for 500 MeV protons. The partial width of the decay $d^* \to NN$ caused by the exchanges of the same mesons is found for this simple model of d^* to be about 9 MeV if the d^* mass is 2100 MeV. The implications of these results are discussed. [S0556-2813(98)04703-7]

PACS number(s): 14.20.Pt, 25.40.Ep

I. INTRODUCTION

The successes of quantum chromodynamics (QCD) between quarks as the fundamental theory of strong interactions have led people to expect new hadronic states often dominated by exotic Fock-space components [1–3]. In nuclear physics, one is particularly interested in new nonstrange dibaryons (with baryon number $A = 2$) of unusually low mass and narrow width that might betray their underlying quark structures. No such dibaryon has been unambiguously identified experimentally despite years of search [3–5].

There are two promising dibaryon candidates, one with unusually high mass and one with unusually low mass. The high-mass candidate is an isospin 1 structure of width not exceeding 80 MeV first seen experimentally in the helicity difference $\Delta \sigma_L(pp)$ of the total pp cross section at an energy that corresponds to a dibaryon mass of 2735 MeV [6]. It has been seen more recently at the same mass in the pp spin correlation parameter A_{00nn} [7].

This structure has been interpreted by Lomon and collaborators [8] as a six-quark "small-bag" state with the nucleon-nucleon (NN) quantum number of $^1S_0$. The interpretation uses the R-matrix formalism to determine if the matching of an internal quark description based on QCD to an external nucleon description based on meson-exchange dynamics at a boundary radius separating the two regions could be made in a way consistent with the empirical NN phase parameters in the neighborhood of the observed structure. (For an assumed quark model of internal wave functions, the resonance energy can be predicted by varying the matching radius r_0 until the external NN wave function vanishes at r_0 at precisely the same c.m. energy as the internal bag-state energy.) The R-matrix analysis also yields a resonance width of about 50 MeV, in rough agreement with experiment. This interpretation will require confirmation by phase-shift analysis or by direct detection via resonance production in nuclear reactions.

In the R-matrix analysis, the experimentally observed mass (2735 MeV) has been found [8] to be consistent with the bag parameters used in the "Cloudy-Bag" model of [9], provided that the pion cloud is neglected. Furthermore, because of its coupling to the external NN channel, the internal bag state is not in equilibrium, and therefore the resonance mass is higher than the equilibrium bag mass of 2680 MeV [10]. If the external pion cloud had been present, as in the actual Cloudy-Bag model [9], the equilibrium mass (at 2380 MeV) would have been much lower [11]. It thus appears that the role of the pion cloud external to the bag needs clarification.

The R-matrix analyses have shown that NN phase parameters are also consistent with many other "high-mass" nonstrange dibaryons [10], such as those predicted by nonrelativistic potential models with pairwise color confinement [12]. It is obvious that the case for these high-mass dibaryons can be significantly strengthened if experimental effects are observed for at least another of these dibaryons. Experimental structures seen in $\Delta \sigma_L(pp)$ at 2900 MeV [13] and in $\Delta \sigma_L(np)$ at 2630 MeV [14] could be candidates for a $^3P_1$ and a $^3S_1$ dibaryon, respectively [15].

In addition, suggestions have been made that these nonstrange dibaryons might appear at much lower masses instead. One with a proposed mass 2065 MeV and width $\Gamma_{\pi NN} = 0.5$ MeV might be responsible for a narrow structure in the energy dependence of the experimental excitation function [at 5° in the center of mass (c.m.)] of the pionic double charge exchange (DCX) reaction $nn(\pi^+, \pi^-)pp$ on nuclear neutrons at $T_{\pi} = 50$ MeV [16]. This explanation seems to be supported by observations of a narrow structure at 2060 MeV with a width < 15 MeV at ITEP [17] and at CELSIUS [18]. The associated dibaryon, usually called d', has the proposed quantum numbers $T = 0$, $J^{\pi} = 0^-$, making it inaccessible from NN channels and consequently narrow. However, an alternative explanation of the DCX phenomenon that requires no dibaryon has also been given [19].

The dibaryon interpretation finds theoretical support in bag models of dibaryon masses where this particular dibaryon appears at 2100 MeV [20] or 2000 MeV [21]. The theoretical bag state involved is a P-wave excitation in the $q^2 - q^4$ separation with the cluster quantum numbers of $(T,S)_{12} = (0,0)$ and $(T,S)_{3456} = (0,1)$. However, in quark potential models with pairwise color confinement, the state appears much higher, at around 2700 MeV [22]. The mass can be reduced considerably with configuration mixing, but it seems difficult to reduce it to below 2400 MeV if one uses quark-quark (qq) dynamics deduced from single-baryon resonances [22].

This paper is concerned with a second nonstrange isoscalar dibaryon called $d*$ which has the quantum numbers $J^\pi = 3^+$, is accessible from $np(^3D_3 - ^3G_3)$ channels, and whose baryon-baryon component is made up of Δ^2. We shall call this $d*$ a didelta when we want to emphasize this Δ^2 component.

The theoretical $d*$ mass $m*$ again covers a wide range: It is highest in the small-bag based R-matrix analysis which yields a value of 2840 MeV [23], well above the $\Delta\Delta$ threshold at 2460 MeV. It is lowest in the quark delocalization and color screening (QDCS) model, where it appears at around 2100 MeV [24–26], just above the πNN threshold at 2020 MeV. Near the lower limit of this mass range, the πNN phase space is small so that the decay of $d*$ is probably dominated there by the NN channel, where the nucleons fall apart in a relative D state. However, the $(\pi)^n NN$ widths could dominate as $m*$ increases.

A search for the $d*$ dibaryon is interesting for the following reasons: In most quark models, the $\Delta - N$ mass difference comes from the color-magnetic term of the one-gluon interaction between pairs of quarks. The total pairwise color-magnetic operator has the same (repulsive) matrix element in $d*$ as in two well separated Δ's if the former's orbital wave-function is totally symmetric in the quark labels [27]. In the Massachusetts Institute of Technology (MIT) bag model [28], the $d*$ mass then falls below the $\Delta\Delta$ threshold by 120 MeV because the spatial integral associated with the interaction is inversely proportional to the bag radius R, and this radius increases from Δ to $d*$ by virtue of the increasing total kinetic energy [1,24]. (The radius of the A-baryon bag of baryon number A is roughly proportional to $A^{1/3}$ in the MIT bag model.)

The situation is different if quark confinement comes from a pairwise qq interaction that rises to infinity at infinite separation. The increasing size of an A baryon containing $3A$ quarks causes its confinement energy to increase so much that the $d*$ mass moves substantially above the $\Delta\Delta$ threshold instead [12]. This result has been confirmed by [29].

The QDCS model is able to reduce the $d*$ mass substantially with the help of two additional assumptions: quark delocalization (QD) and color screening (CS) [24–26]. QD takes advantage of the fact that the kinetic energy of a single quark state could be reduced if it is partly on the left side and partly on the right side of the system. For a Gaussian spatial wave function, a maximum reduction of the kinetic energy of about 19% appears when there is a 50/50 left/right separation with the two wave function centers separated by 2.3 oscillator lengths, like two peas in a pod. For a dibaryon built up of a product of six such delocalized quark wave functions, about 72% of the system is in the cluster configurations of the type $q^2 - q^4$ and $q - q^5$ where the reduction in the kinetic energy can be realized. If one reduces the total kinetic energy in the MIT bag by the resulting 14% (72% of 19%), one gets a $d*$ mass of about 2090 MeV instead of the usual 2340 MeV, assuming that the interaction and confinement energies retain their spherical forms.

However, in color confinement models or even in string models, this QD reduction of the kinetic energy alone cannot overcome the strong increase in pairwise color confinement energy with increasing qq separations and with increasing baryon number A. Color screening now comes into play by assuming that the rising repulsion of the confinement potential at large distances [12] does not exceed a finite upper bound [24,29]. Now finally QD could become energetically favorable in A baryons. (The model of [26] achieves the same result by measuring the confinement energy from the nearer baryon center, thus avoiding large qq separations.)

The QD phenomenon could presumably be restricted to the interior of a bag. However, if realized between well-separated baryons [25], the idea has far-reaching implications. With quark delocalization taking place at all densities, the transition to the quark-gluon plasma will be at best a second-order phase transition. This seems to imply that if such an extreme picture is correct, attempts to search for quark-gluon plasmas might be doomed to failure, given the difficulty of detecting unambiguous signals from even a first-order phase transition. However, a counter-argument is provided by the recent observation of unusually strong absorption of J/ψ mesons in Pb-Pb collisions [30]. One interpretation [31] is that this is a signal for the color deconfinement phase transition [32]. Consequently, it would be interesting to look for experimental indications for or against the QDCS model. This cannot be done by studying nuclear forces, which can already be understood in terms of meson exchanges. In contrast, the observation of a low $d*$ mass could be taken as a signal for QD in A baryons.

In this connection, it is worth noting that a recent R-matrix analysis of available NN phase shifts below the dibaryon mass of 2240 MeV finds no sign of a $d*$ resonance in the $np(^3D_3 - ^3G_3)$ channels with a width greater than 1 MeV [15]. However, the analysis does not exclude a narrower $d*$ at a mass in between the energies of known phase shifts.

In any case, progress in our understanding of dibaryons will require new experimental inputs. In particular, any new information on whether the $d*$ mass might be high or low is likely to have important implications on the dynamics of quark confinement in baryons.

The dibaryon $d*$ could be produced by the inelastic scattering of projectiles from nuclear targets. The understanding of past failures to find it [4,5] and the justification for future searches in such reactions would require some theoretical input concerning its production and decay properties. The main purpose of this paper is to explore how its production cross section in pd inelastic scattering and its partial decay width into two nucleons could be calculated using standard techniques in nuclear reactions and a simple model of the $d*$ as a didelta object. Some of the issues which must be resolved before realistic results can be obtained are briefly discussed.

II. THE $pd \rightarrow pd*$ PRODUCTION CROSS SECTION

In our treatment of the inelastic production, the $d*$ is taken to be a pure Δ^2 Gaussian wave function with an average $\Delta\Delta$ separation of $2r* = 1.4$ fm [24–26]. No D-state or hidden-color components are included. Consistent with such a crude $d*$ wave function, the deuteron is also crudely aproximated by an S-state wave function made up of a sum of three Gaussians fitted to the Bonn C S-state wave function [33] renormalized back to 100%. The quark wave function in each baryon is assumed to be the same in both N and Δ with

a quark-model r.m.s. radius of $r_p = 0.6$ fm [24]. The quarks in each baryon are localized to the left or right Δ in d^*, with no left-right antisymmetrization or delocalization [24] yet included. Later in the paper, we shall estimate qualitatively the effects of delocalization in the calculated quantities.

The excitation of $d(T=0,1^+)$ to $d^*(T=0,3^+)$ requires an isoscalar transfer of 2 units of angular momentum. In the usual models of nuclear forces containing the exchanges of only pseudoscalar, scalar and vector mesons, d^* can only be reached in the lowest order by a spin-isospin flip in each of the two target nucleons. Each spin-isospin flip is caused by the exchange of an isovector meson such as π and ρ between the projectile and the target nucleon. It will turn out that the unpolarized cross section has important contributions from that part of the NN t-matrix proportional to the operator $(\boldsymbol{\sigma}_A \cdot \mathbf{q})(\boldsymbol{\sigma}_B \cdot \mathbf{q})(\boldsymbol{\tau}_A \cdot \boldsymbol{\tau}_B)$, where A, B are nucleon labels.

The spin-averaged differential cross section in the c.m. frame has the structure

$$\frac{d\sigma_{\mathrm{fi}}}{d\Omega^*} = \frac{p_i^* p_f^*}{\pi} \frac{d\sigma_{\mathrm{fi}}}{dt} = p_i^* p_f^* \langle |\mathcal{A}_{\mathrm{fi}}|^2 \rangle_{\mathrm{spin}}, \quad (1)$$

where p_α^* is the proton momentum in the reaction c.m. frame in the initial or final reaction state α. The invariant inelastic amplitude

$$\mathcal{A}_{\mathrm{fi}}(\mathbf{q}) \approx \left(\frac{iN_{\mathrm{T}}}{2\pi} \right) \int S_{\mathrm{fi}}(\mathbf{q}') \left[\frac{f_1(\mathbf{q}_1)}{k^*} \frac{f_2(\mathbf{q}_2)}{k^*} \right] F_{\mathrm{B}}^2(\mathbf{q}_1) F_{\mathrm{B}}^2(\mathbf{q}_2)$$

$$\times \sum_{i=1,2} N_{\mathrm{P}i} S_{\mathrm{BB}i}(\mathbf{q},\mathbf{q}') d^2\mathbf{q}' \quad (2)$$

is approximated by the Glauber double-scattering contribution [34] between quarks in the c.m. frame of the reaction. Each scattering changes a target nucleon into a Δ. The integral involves two momentum transfers

$$\mathbf{q}_1 = \frac{1}{2} \mathbf{q} + \mathbf{q}', \quad \mathbf{q}_2 = \frac{1}{2} \mathbf{q} - \mathbf{q}'. \quad (3)$$

The inelastic form factor $S_{\mathrm{fi}}(\mathbf{q})$ from the baryon wave functions of the initial and final dibaryon states will be constructed from the S-wave Δ^2 wave function of d^*:

$$\psi_{\mathrm{f}}(\mathbf{p}) = \mathrm{const} \exp\left(-\frac{p^2}{2\beta^{*2}} \right), \quad (4)$$

where $\mathbf{p}$ is the relative baryon momentum and $\beta^* = \sqrt{(3/8)}/r^*$. The deuteron wave function used contains Gaussians of the form

$$\psi(\mathbf{p}) = \mathrm{const} \exp\left(-\frac{p^2}{2\beta^2} \right), \quad (5)$$

where the parameters β will be given later. Hence the inelastic wave function form factor is a sum of terms each of the form

$$S_{\mathrm{fi}}(\mathbf{q}) = \left(\frac{2\beta\beta^*}{\beta^2 + \beta^{*2}} \right)^{3/2} \exp\left[-\frac{q^2}{2(\beta^2 + \beta^{*2})} \right]. \quad (6)$$

There are additional ''baryon'' form factors coming from the internal quark structure of baryons.

The dynamical description is simplest if it is first brought down to the quark level. Then an outside factor $N_{\mathrm{T}} = 9$ appears in Eq. (2) giving the number of distinct quark pairs on the target side, with one quark from each of the two target baryons. The contribution on the projectile proton side is slightly more complicated. There is a contribution from $N_{\mathrm{P1}} = 3$ projectile quarks each interacting twice with the target, and an effective contribution from three pairs of projectile quarks of

$$N_{\mathrm{P2}} = 3 \left\langle \frac{1}{9} (\boldsymbol{\sigma}_1 \cdot \boldsymbol{\sigma}_2)(\boldsymbol{\tau}_1 \cdot \boldsymbol{\tau}_2) \right\rangle_P = \frac{5}{3}, \quad (7)$$

where the expectation value of the operators of quarks 1 and 2 in the projectile (P) is taken over the quark wave function of the projectile proton.

The inelastic baryon form factor involved is different in each of these two cases, being both different from the elastic formfactor F_{B}^2 for NN scattering. Eventually we shall reconstruct NN amplitudes from the quark-quark (qq) amplitudes f_i. For this reason, it is useful to separate each inelastic baryon formfactor into an elastic factor F_{B}^2 and an inelastic correction:

$$S_{\mathrm{BB1}}(\mathbf{q},\mathbf{q}') = \exp\left[-\frac{q^2}{12b^2} + \frac{q'^2}{3b^2} \right], \quad (8)$$

$$S_{\mathrm{BB2}}(\mathbf{q},\mathbf{q}') = \exp\left[\frac{q^2}{24b^2} - \frac{q'^2}{6b^2} \right], \quad (9)$$

where $b = 1/r_p$. These have been calculated from the assumed Gaussian wave function of a baryon ($B = N$ or Δ) made up of quarks 1–3:

$$\phi_{\mathrm{B}}(\boldsymbol{\rho}_{12}, \boldsymbol{\lambda}_{123}) = \mathrm{const} \exp\left[-\frac{1}{2b^2}(\rho_{12}^2 + \lambda_{123}^2) \right], \quad (10)$$

where

$$\boldsymbol{\rho}_{12} = (\mathbf{p}_1 - \mathbf{p}_2)/\sqrt{2}, \quad \boldsymbol{\lambda}_{123} = (2\mathbf{p}_3 - \mathbf{p}_1 - \mathbf{p}_2)/\sqrt{6}. \quad (11)$$

The theoretical elastic form factors F_{B} are also Gaussians, but they will be absorbed into the empirical NN scattering amplitudes that will eventually appear. They do not appear explicitly in our final formula.

The momentum k^* is the NN relative momentum in the NN c.m. frame. For elastic scattering, or in the high-energy limit where the inelasticity is negligibly small, it is sufficient to use the elastic scattering value $k_{\mathrm{el}} = (3/4)p_i^*$. We recognize that in inelastic scattering at lower energies, the effect of the smaller projectile momentum p_f^* in the final state should be taken into consideration, in order to describe more accurately the energy dependence of both kinematics and dynamics. One possibility is to use the geometrical mean momentum $(3/4)\sqrt{p_i^* p_f^*}$, but this cannot be correct because it gives the wrong behavior at threshold. Of course, the Glauber multiple-diffraction formalism is a high-energy approximation that should not be used too close to a reaction threshold, but it is conceptually also important to ensure that the invari-

ant amplitude $\mathcal{A}$ does not have a spurious singularity at threshold. The threshold behavior is not just a question of kinematics, because the elementary amplitude $f_i(\mathbf{q})$ is also involved.

Now the inelastic production of d^* involves at least two collisions. At each collision, the energy transfer can have a range of values. This suggests that the correct description might require an average over some distribution. We shall use the simplest realization of this concept, namely the assumption that the NN dynamics in Eq. (2) should be that for the arithmetical average of the proton energies in the initial and final states:

$$T_{av} = T_{lab} - \frac{1}{2}\Delta m^*, \qquad (12)$$

where $\Delta m^* = m^* - m_d$ is the mass transfer in the inelastic scattering. The momentum k^* is the relative momentum in the NN c.m. frame when a proton projectile of kinetic energy T_{av} is incident on a nucleon target:

$$k^* = \sqrt{\frac{1}{4}s_{NN} - m^2}, \qquad (13)$$

where $s_{NN} = 2m(2m + T_{av})$ is the squared c.m. energy of the two nucleons each of mass m. In this prescription, the Glauber double-scattering integral for the invariant amplitude does not show a spurious singularity at threshold.

The dynamical factors (f_i/k^*) inside the Glauber double-scattering integral is approximately frame invariant, because in the usual parametrization using the optical theorem, it depends primarily on the total NN cross section σ_{NN} if nucleons were the elementary objects of the Glauber method.

There are qq operators hidden in the qq scattering amplitudes f_i in Eq. (2). These quark scattering amplitudes are constructed from empirical NN scattering amplitudes by using known relations between nucleon and quark operators [35]. The reduction of NN amplitudes involving the NN operator $(\boldsymbol{\sigma}_A \cdot \mathbf{q})(\boldsymbol{\sigma}_B \cdot \mathbf{q})(\boldsymbol{\tau}_A \cdot \boldsymbol{\tau}_B)$, where A, B are nucleon labels, requires a number of steps:

(a) We first use the well-known relation [35] $g_{mqq} = (3/5)g_{mNN}$, where m is π or ρ.

(b) The qq operators are simplified by using the identities

$$(\boldsymbol{\sigma} \cdot \mathbf{q}_1)(\boldsymbol{\sigma} \cdot \mathbf{q}_2) = \mathbf{q}_1 \cdot \mathbf{q}_2 + i\boldsymbol{\sigma} \cdot (\mathbf{q}_1 \times \mathbf{q}_2), \qquad (14)$$

$$(\boldsymbol{\sigma}_i \cdot \mathbf{q}_1)(\boldsymbol{\sigma}_j \cdot \mathbf{q}_2)$$
$$= \frac{1}{3}(\boldsymbol{\sigma}_i \cdot \boldsymbol{\sigma}_j)(\mathbf{q}_1 \cdot \mathbf{q}_2) + \frac{1}{2}(\boldsymbol{\sigma}_i \times \boldsymbol{\sigma}_j) \cdot (\mathbf{q}_1 \times \mathbf{q}_2)$$
$$+ (\boldsymbol{\sigma}_i \times \boldsymbol{\sigma}_j)^{(2)} \cdot (\mathbf{q}_1 \times \mathbf{q}_2)^{(2)}. \qquad (15)$$

Only the tensor-force terms involving $(\boldsymbol{\sigma}_6 \times \boldsymbol{\sigma}_9)^{(2)}(\boldsymbol{\tau}_6 \cdot \boldsymbol{\tau}_9)$ for two target quarks 6 and 9 contribute to d^* production. (Quarks 4–6 are in the first target baryon, while 7–9 are in the second.) On the projectile side (involving quarks 1–3), we keep only the term that is spin-independent. A projectile spin-orbit term can be shown not to contribute to the spin-averaged production cross section under rather general circumstances.

The identity (15) can also be used to handle central spin-isospin dependent interactions by replacing one or more of the momentum transfers $\mathbf{q}_m$, $m = 1,2$, from the tensor interactions by projectile quark spin operators $\boldsymbol{\sigma}_m$, $m = 1,2$, of the central interactions. In this way, one can show that when both interactions are central, the production of d^* involves the spin operator $(\boldsymbol{\sigma}_6 \times \boldsymbol{\sigma}_9)^{(2)} \cdot (\boldsymbol{\sigma}_1 \times \boldsymbol{\sigma}_2)^{(2)}$. We see that the projectile part of this operator induces 2 units of spin transfer at the projectile, which cannot then remain a proton. However, the production $pd \rightarrow pd^*$ is possible when one interaction is central and the other is tensor, because in this case the projectile operator is of the form $(\boldsymbol{\sigma}_1 \times \mathbf{p}_2)^{(2)}$. The projectile then suffers only 1 unit of spin transfer. This mixed tensor-central contribution will not be included in the present exploratory study.

(c) In the result reported here, we have neglected all quark-exchange terms between target baryons. This permits the required operator matrix elements to be calculated in terms of the reduced matrix element

$$((N^2)S'T' = 10\|(\boldsymbol{\sigma}_6 \times \boldsymbol{\sigma}_9)^{(2)}(\boldsymbol{\tau}_6 \cdot \boldsymbol{\tau}_9)\|(\Delta^2)30) = \frac{16}{9}\sqrt{\frac{7}{2}}. \qquad (16)$$

Results with fully antisymmetrized quark wave functions for the target will be reported elsewhere when completed.

On the other hand, the use of NN t-matrices ensures that all quark exchanges between projectile and target nucleons are automatically included.

(d) The spin-orbit terms in the NN amplitude are neglected, as we are not concerned here with polarization phenomena.

The spin-averaged differential production cross section then takes the form

$$\frac{d\sigma_{fi}}{d\Omega^*} = \left(\frac{1}{15}\right)\sum_{\mu = -2}^{2}|\mathcal{F}_\mu(\mathbf{q})|^2, \qquad (17)$$

where

$$\mathcal{F}_\mu(\mathbf{q}) = \frac{C}{\pi}\int d^2\mathbf{q}'\sum_{i=1,2}N_{Pi}S_{BBi}(\mathbf{q},\mathbf{q}')h(\mathbf{q},\mathbf{q}')$$
$$\times\left[\frac{1}{4}(\mathbf{q}\times\mathbf{q}) - (\mathbf{q}'\times\mathbf{q}')\right]_{-\mu}^{(2)}, \qquad (18)$$

$$C = \left(\frac{N_T}{2k^{*2}}\right)\left(\frac{3}{5}\right)^4\left(\frac{16}{9}\right)\sqrt{\frac{7}{2}}, \qquad (19)$$

$$h(\mathbf{q},\mathbf{q}') = \left(\frac{1}{4}q^2 - q'^2\right)\left(\frac{m}{4\pi}\right)t_{ivt}(\mathbf{q}_1)t_{ivt}(\mathbf{q}_2)S_{fi}(\mathbf{q}'). \qquad (20)$$

We shall use the empirical NN isovector-tensor (IVT) t-matrix t_{ivt} constructed from NN phase shifts by Franey and Love (LF) [36]. The one appearing here is actually three times the tensor-force function tabulated by LF, i.e., the NN scattering amplitude is here defined as

$$f_{NN}(\mathbf{q}) = -\left(\frac{m}{4\pi}\right)t_{NN}(\mathbf{q}) = \left(\frac{m}{4\pi}\right)t_{ivt}(q)(\boldsymbol{\sigma}_1 \cdot \mathbf{q})(\boldsymbol{\sigma}_2 \cdot \mathbf{q})$$
$$\times(\boldsymbol{\tau}_1 \cdot \boldsymbol{\tau}_2) + \cdots, \qquad (21)$$

where the tensor operator is 1/3 of that contained in the usual tensor-force operator used in nuclear physics.

In the Born approximation, $t_{NN}(\mathbf{q})$ simplifies to the Fourier transform $V(\mathbf{q})$ of the NN potential in the notation of Ref. [33]. In fact, we shall also use the Full Bonn potential [33] in the Born approximation to study the separate contributions of π and ρ exchanges and the dependence of the production cross section on the projectile energy.

For the deuteron target, we use the Bonn C deuteron S-state wave function after fitting it to the nonorthogonal three-term Gaussian form

$$\psi_{\text{Bonn C}}(p) \approx \sum_{i=1}^{3} c_i \psi_i(p), \qquad (22)$$

where $\psi_i(p)$ is a normalized S-state oscillator wave function. The resulting range parameters obtained by minimizing the *percentage* m.s. deviation are

$$\gamma = (\gamma_1, \gamma_2, \gamma_3) = 0.04467(1, 5.04, 21.5) \text{ fm}^{-2}, \quad (23)$$

where $\gamma_i = 2\beta_i^2$. The expansion coefficients, renormalized from the fitted value of 94.34% back to 100%, are

$$\mathbf{c} = (c_1, c_2, c_3) = (0.31491, 0.49716, 0.36926). \quad (24)$$

This is an excellent fit to the Bonn C deuteron S-wave function whose probability is 94.39%.

The momentum transfer $\mathbf{q}$ of the reaction is of course calculated with the correct (relativistic) inelastic kinematics. However, the other momentum transfers of the Glauber approximation are treated in the high-energy limit where the inelasticity is negligibly small. As is known, the z-axis of the Glauber formula is usually not constant in space but chosen instead along the bisector of the initial- and final-state momenta. This means that the momentum transfer is on the equatorial, or xy, plane. In fact, all momenta in the Glauber double-scattering formula lie on this equatorial plane. In extending the formula to inelastic scattering, we have kept all momenta on the equatorial plane even when the energies involved are not very high. This means that two of the terms in the sum in Eq. (17), namely for $\mu = \pm 1$, are zero.

III. RESULTS FOR THE PRODUCTION CROSS SECTION

The results shown in this section are all calculated in that angle-averaged approximation in which $\cos\theta'$ everywhere inside the integrand in Eq. (2) is taken to be $1/\sqrt{2}$, θ' being the angle between $\mathbf{q}$ and $\mathbf{q}'$. The effect of a full angle integration will be discussed near the end of this section. For the sake of completeness, we shall give full angular distributions even though the Glauber multiple-diffraction approximation is known to be reliable only for small angles.

Figure 1 gives the differential production cross sections at the TRIUMF proton energy of 516 MeV. The 1985 Love-Franey (LF) t-matrix [36] at the lab energy of 515 MeV (on a nucleon target) is used for d^* masses of $m^* = 2050$, 2100, and 2150 MeV, a range of particular interest for the QDCS model mentioned in the Introduction. Calculated with the same NN t matrix, these cross sections involve exactly the same invariant production amplitude. They differ only in the outside kinematical factors $p_i^* p_f^*$ in Eq. (1) and in the fact
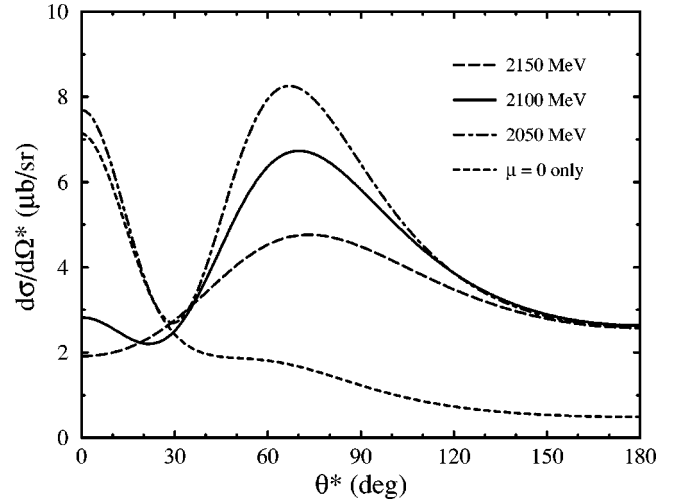

FIG. 1. Center-of-mass differential cross section for $pd \to pd^*$ at the proton lab energy of 516 MeV for different d^* masses m^* using the 1985 Love-Franey t-matrix at 515 MeV. The $m^* = 2050$ MeV result from only the $\mu = 0$ term of Eq. (9) is also shown.

that the angular distribution covers a narrower range in momentum transfer as m^* increases. For this reason, it is often necessary to show results for only the smallest $m^* = 2050$ MeV because it has the largest range of momentum transfers.

The cross sections shown are about 7 μb/sr at the second maximum at about 70° c.m.. They decrease with increasing d^* mass, and should vanish at threshold. The structure at small angles, seen very clearly in the $m^* = 2050$ MeV result, comes from the $\mu = 0$ component of the production tensor operator. Its contribution to the differential cross section of Eq. (17) for $m^* = 2050$ MeV is shown separately as a short dashed curve in Fig. 1. The remaining contributions are from the $\mu = \pm 2$ components. Being proportional to q^4 for small q^2, they are responsible for the second maximum. The strong μ dependence means that the angular distributions can be expected to be very different when the colliding particles are polarized.

The production mechanism, requiring at least a double scattering, is particularly sensitive to the dynamics of the effective qq tensor force, here derived from the empirical NN tensor force. It is therefore of interest to show, in Fig. 2, how strongly the production cross section for $m^* = 2050$ MeV at the TRIUMF energy increases as the effective nucleon lab energy of the input NN t-matrix is decreased.

Since the production cross section as calculated depends only on the isovector tensor part of the NN t-matrix, the effect seen is a direct reflection of the latter's rapid increase with decreasing nucleon energy. This behavior is well understood in the theory of nuclear forces: The shorter-range part of the tensor force due to the exchange of ρ mesons is opposite in sign to the longer-range part from π exchange. As the scattering energy decreases, the strong and long-range π-exchange contribution becomes rapidly more dominant. We shall be able to show separately the results calculated from each of these two parts of the NN tensor force when we use the Full Bonn potential.
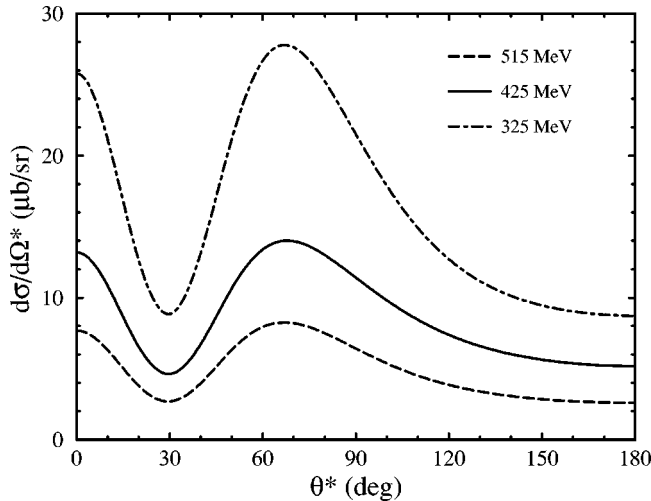
FIG. 2. Differential cross sections for $pd \to pd^*$ at 516 MeV for different Love-Franey t-matrix energies using $m^* = 2050$ MeV.

The inelasticity involved in d^* production for the m^* range examined here is a very appreciable fraction of the energy available in the beam. Given the strong dependence of the production cross section on the effective nucleon energy of the NN isovector tensor t matrix, it is necessary to choose this energy carefully. For reasons discussed in the last section, we shall use the average lab energy T_{av} shown in Eq. (12) which is the arithmetical average over the initial and final states.

The resulting cross sections for different d^* masses are shown in Fig. 3. These are obtained by interpolating the results calculated for the three lab energies $T = 515$, 425, and 325 MeV tabulated by LF. We see that interpolated results have increased by a factor of about 2.0 over the value calculated at the incident energy for $m^* = 2100$ MeV. The final cross sections at the second maximum are about 13 μb/sr. This is very large, but it is perhaps not totally unexpected because the production involves the same amplitudes responsible for the resonance production of Δ from nucleon targets.

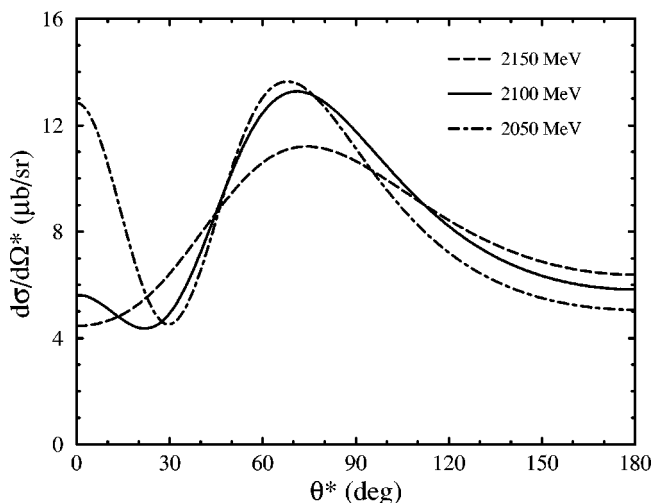The use of empirical t matrices takes care of rescattering

FIG. 3. Differential cross sections for $pd \to pd^*$ at 516 MeV for different m^* masses using the Love-Franey t matrix at the energy averaged over the initial and final states.
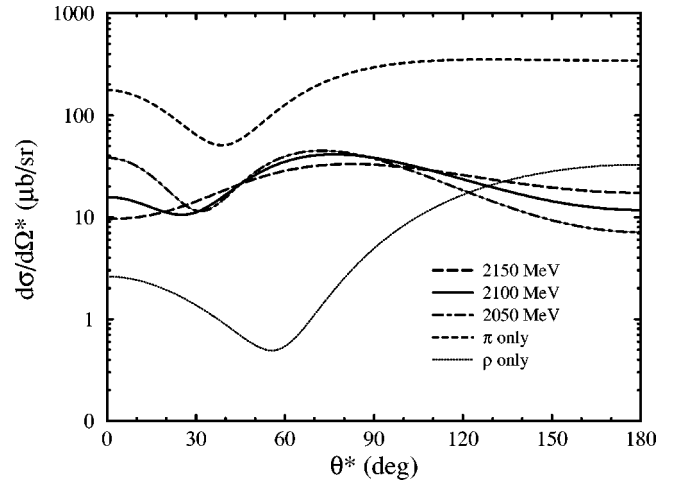

FIG. 4. Differential cross sections for $pd \to pd^*$ at 516 MeV for different m^* in the notation of Fig. 3 using the Full Bonn potential in the Born approximation with the NN relative momentum k^* calculated at an average energy T_{av}. The $m^* = 2050$ MeV results for π exchange only and for ρ exchange only are also given.

or wave-distortion effects in the sense of an impulse approximation. To determine how important such effects are, we use the full Bonn potential treated in the Born approximation. The results obtained with the NN relative momentum k^* shown in Eq. (2) calculated from T_{av} are shown in Fig. 4 for different values of m^*.

We see that these production cross sections have the same angular behavior as those in Fig. 3 for the LF t-matrix, but their values are higher by a factor of about 2.8. The effect might seem huge, but since the calculated cross section is proportional to g^8, where g is a meson-NN coupling constant, the t-matrix reduction of the effective g^2 is by a very modest factor of 0.77. In other words, a strong sensitivity to NN dynamics is unavoidable in such a high-order production process. A quantitative calculation of the cross section might well require better t matrices constructed from more recent NN phase shifts.

The use of the Bonn potential allows the contributions of the π- and ρ-exchange potentials to be separated. The cross sections for each contribution alone are also shown in Fig. 4. Note that their total contribution to the cross section is not the sum of their separate contributions because amplitudes interfere and the production mechanism is double scattering. The π-only result is enormous, but it is effectively controlled by the much weaker ρ exchange contribution. Since this cancellation is not a well-determined part of NN dynamics, Fig. 4 also shows the importance of using the best NN input in the calculation.

The Born approximation should improve in accuracy with increasing projectile energy. Figure 5 shows how the calculated cross section for $m^* = 2050$ MeV decreases with increasing energy, while the second maximum moves forward in the angular distribution, but not in the momentum transfer. Both features are consistent with the expected energy dependence of cross sections. Of course, the accuracy of the Bonn potential at these higher energies is somewhat uncertain. In spite of this reservation, Fig. 5 does suggest that the production cross section will not decrease sharply with increasing energy.
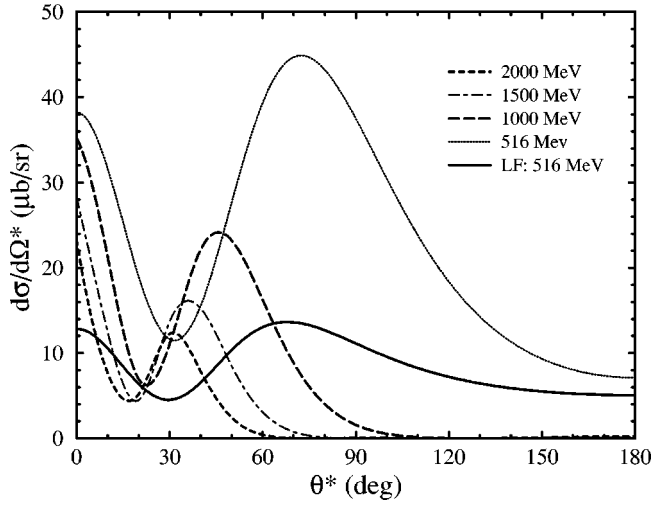
FIG. 5. Differential cross sections for $pd \to pd^*$ for different projectile energies using $m^* = 2050$ MeV, the Full Bonn potential in the Born approximation, and an average nucleon energy T_{av}.

The production cross section also depends on the d^* wave function size r^* (half of the average $\Delta\Delta$ separation). Figure 6 gives the results calculated for $r^* = 0.5, 0.7, 0.9$ fm, covering a realistic range of possible d^* sizes. Other parameters used are $m^* = 2050$ MeV and an effective nucleon energy of 425 MeV for the LF t matrix, very close to the recommended average value of 429 MeV. We see that the effect is fairly strong especially for smaller d^*'s presumably because the momentum transfers involved can then be more different. We therefore conclude that the calculated cross section can be quite sensitive to the short-range components of the wave functions of both d and d^*. The short-range components neglected in the present calculation include the deuteron D state, exotic admixtures, and the effects of quark exchange and delocalization.

Finally, we address the question of the accuracy of the angle-averaged approximation used this section. A selected number of angle-integrated cross sections for the TRIUMF energy using the Bonn potential with $m^* = 2050$ MeV have
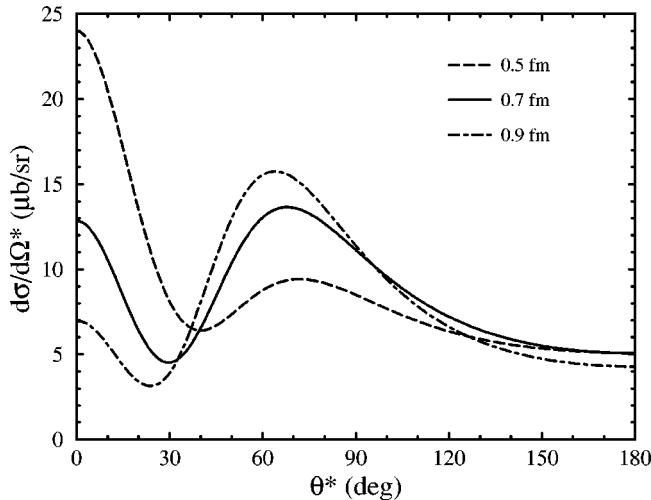

FIG. 6. Differential cross sections for $pd \to pd^*$ at 516 MeV for different d^* wave-function radii r^* for $m^* = 2050$ MeV using the Love-Franey t matrix at 425 MeV.

been calculated. The angle-integrated result at the CM angle $\theta^* = 70(0,180)^\circ$ is 47.21 (37.08, 7.140) μb/sr when the angle-averaged approximation gives 44.71 (38.20, 7.118) μb/sr instead. Thus the angle-averaged approximation seems to have adequate accuracy.

The present calculations have given only a crude picture of the inelastic production of d^*. Their many limitations will be discussed in the last section.

IV. THE $d^* \to NN$ DECAY WIDTH

The dibaryon d^* cannot decay into two nucleons if its constituents do not interact. The simplest interaction that can do it is a two-quark interaction containing the spin operator $(\boldsymbol{\sigma}_i \times \boldsymbol{\sigma}_j)^{(2)}$, to bridge the gap between initial and final intrinsic spins. If d^* is a didelta, even when these deltas are not pointlike, the perturbing operator must also contain the isospin operator $\boldsymbol{\tau}_i \cdot \boldsymbol{\tau}_j$ in order to change a Δ into an N at each quark vertex. It is clear that isospin-independent interactions cannot do it. Thus all direct gluon exchanges do not contribute, no matter how strong they are.

Among the simplest two-quark interactions that can do it are the one-meson-exchange potentials carried by π and ρ. We shall show below that their contributions are quite large.

It can be argued that these mesons might not have the presence inside d^* that they have in the outside meson cloud, because much of the dibaryon interior might be in a different vacuum state, the so-called perturbative QCD vacuum, where mesons loose their individuality. Since QCD is flavor-independent, the required $\boldsymbol{\tau}_i \cdot \boldsymbol{\tau}_j$ operator could only come from the Heisenberg isospin exchange operator

$$\mathcal{P}^\tau = \frac{1}{2}\left(1 + \boldsymbol{\tau}_i \cdot \boldsymbol{\tau}_j\right) \qquad (25)$$

arising from the Pauli exchange of two quarks. We now show that the resulting potential has a functional form similar to that for one-meson exchange. In this preliminary study, we shall not consider any three-quark interactions, including those where two interacting quarks involve a noninteracting quark via Pauli exchange, because they have more complicated structures.

The exchange two-quark interaction generated by one-gluon exchange (OGE) between quarks i,j can be written in the familiar form [37,38]

$$V_{xqq} = -\mathcal{P}_{ij}V_{qq} = -\mathcal{P}^\lambda\mathcal{P}^\tau\mathcal{P}^\sigma\mathcal{P}^x V_{qq}, \qquad (26)$$

where

$$\mathcal{P}^\lambda = \frac{1}{2}\left(\frac{2}{3} + \boldsymbol{\lambda}_i \cdot \boldsymbol{\lambda}_j\right) \qquad (27)$$

is the color exchange operator. The space exchange operator $\mathcal{P}^x$ interchanges the spatial labels in the qq final state. For an exchanged gluon of effective mass μ, the direct qq interaction from OGE has the standard one-boson-exchange form [33]

$$V_{qq}(\mathbf{q}) = \frac{V_0}{\mu^2 + q^2} (\boldsymbol{\lambda}_i \cdot \boldsymbol{\lambda}_j)[-(\boldsymbol{\sigma}_i \cdot \boldsymbol{\sigma}_j)q^2$$

$$+ (\boldsymbol{\sigma}_i \cdot \mathbf{q})(\boldsymbol{\sigma}_j \cdot \mathbf{q}) + \cdots]. \qquad (28)$$

The QCD coupling constant appearing in V_0 is dependent on the gluon mass μ. In addition, it should be an effective coupling constant that might include certain higher-order effects.

Of the terms shown, the second term is a tensor interaction which tends to be unobtrusive in baryon spectroscopy, just like tensor forces in nuclear spectroscopy. However, the first term is the color-magnetic interaction which can be related to the $\Delta - N$ mass difference $\Delta m = m_\Delta - m_N = 293$ MeV:

$$V_0 = \frac{\Delta m}{16 I_B}. \qquad (29)$$

Here

$$I_B = \int d^3\mathbf{q} \left\langle \frac{q^2}{q^2 + \mu^2} \delta_i \delta_j \right\rangle \qquad (30)$$

is the spatial two-quark matrix element in a baryon (B), taken for simplicity to be the same in both Δ and N. There are momentum-conserving δ-functions δ_k for the two quarks i, j at each gluon-quark-quark vertex.

Is this empirical qq interaction strong or weak? This question can be answered by anticipating that even though both V_0 and the gluon propagator in V_{qq} depend significantly on the gluon mass μ, their effects tend to cancel when the same $\Delta - N$ mass difference is fitted. The interaction strength V_0 turns out to be 0.11 GeV^{-2} when μ is taken to be the ρ meson mass. In contrast, the equivalent strength of the one-rho-exchange (ORE) potential in the full Bonn potential is

$$V_0 = \left(\frac{3}{5}\right)^2 \frac{\pi}{m^2} \frac{g_\rho^2}{4\pi} \left(1 + \frac{f_\rho}{g_\rho}\right)^2 = 54 \text{ GeV}^{-2}, \qquad (31)$$

where the factor $(3/5)^2$ comes from the reduction from NN to qq operators. This is about 500 times stronger than the qq interaction strength. Although the ρNN coupling constants are not well determined in the NN interaction, it is clear that the ORE potential appropriate to the baryon exterior is some two orders of magnitude stronger than the effective qq interaction present in the perturbative vacuum of the baryon interior. This shows that the OGE contribution to the partial decay width is negligibly small compared to the meson-exchange contributions.

It is nevertheless interesting to complete the derivation of the exchange qq interaction and to determine how the space-exchange operator $\mathcal{P}^x$ further affects the final result. We therefore go on by noting that the term in V_{xqq} containing the $d^* \to NN$ decay operator can be isolated by using the expansion

$$-\mathcal{P}^\lambda \mathcal{P}^\tau \mathcal{P}^\sigma (\boldsymbol{\lambda}_i \cdot \boldsymbol{\lambda}_j)(\boldsymbol{\sigma}_i \cdot \mathbf{q})(\boldsymbol{\sigma}_j \cdot \mathbf{q})$$

$$= -\frac{8}{9}(\boldsymbol{\sigma}_i \cdot \mathbf{q})(\boldsymbol{\sigma}_j \cdot \mathbf{q})(\boldsymbol{\tau}_i \cdot \boldsymbol{\tau}_j) + \cdots, \qquad (32)$$

obtained with the help of the identities

$$(\boldsymbol{\lambda}_i \cdot \boldsymbol{\lambda}_j)^2 = \frac{32}{9} - \frac{4}{3}(\boldsymbol{\lambda}_i \cdot \boldsymbol{\lambda}_j) \qquad (33)$$

and

$$(\boldsymbol{\sigma}_i \cdot \boldsymbol{\sigma}_j)(\boldsymbol{\sigma}_i \cdot \mathbf{q})(\boldsymbol{\sigma}_j \cdot \mathbf{q}) = (\boldsymbol{\sigma}_i \cdot \mathbf{q})(\boldsymbol{\sigma}_j \cdot \mathbf{q}) + (1 - \boldsymbol{\sigma}_i \cdot \boldsymbol{\sigma}_j)q^2. \qquad (34)$$

The final result is

$$V_{xqq}(\mathbf{q}) = -\mathcal{P}^x\left(\frac{8}{9}\right)(\boldsymbol{\sigma}_i \cdot \mathbf{q})(\boldsymbol{\sigma}_j \cdot \mathbf{q})(\boldsymbol{\tau}_i \cdot \boldsymbol{\tau}_j) \frac{V_0}{\mu^2 + q^2} + \cdots, \qquad (35)$$

showing only the term which can turn colorless Δ's into colorless N's. This term too has a strength characterized by V_0. This is the only term that can contribute, in the lowest order, to the decay of the d^* treated as a didelta.

In more realistic models of d^*, colored Δ's appear in the so-called "hidden-color" components [39]. These colored objects can decay into NN by both direct and exchange OGE potentials via terms proportional to the color operator $\boldsymbol{\lambda}_i \cdot \boldsymbol{\lambda}_j$. However, all such contributions are necessarily based on the effective qq interaction V_{qq} whose strength V_0 is two orders of magnitude weaker than meson-exchange interactions.

We are now in a position to calculate the decay width. Its spin-averaged value in first-order perturbation theory [40] has the structure

$$\Gamma(m^*) = 2\pi p^* \mu_f^* \int d^2\Omega_{\mathbf{p}^*} |N_{qq}\langle(N^2)\mathbf{p}^*|V|(\Delta^2)d^*\rangle|^2_{\text{spin}}, \qquad (36)$$

where $\mathbf{p}^*$ is a nucleon momentum in the center-of-mass frame and μ_f^* ($= m^*/4$) is the relativistic reduced mass in the final state calculated with dynamical masses or total energies. $N_{qq} = 9$ pairs of qq interaction V contribute to the decay. The momentum state $|\mathbf{p}^*\rangle$ has the normalization:

$$\langle\mathbf{r}|\mathbf{p}^*\rangle = \frac{1}{(2\pi)^{3/2}} e^{i\mathbf{p}^* \cdot \mathbf{r}}. \qquad (37)$$

After some algebra, the decay width can be written in the final form

$$\Gamma(m^*) = \frac{p^* \mu_f^*}{7}\left[N_{qq} \frac{16}{9} \sqrt{\frac{7}{2}}\right]^2 \frac{16}{15}$$

$$\times \frac{1}{(2\pi)^2 \pi^{3/2}}\left(\frac{\beta^{*7}}{\kappa^6}\right)|F_{\text{model}}|^2, \qquad (38)$$

where the model-dependent factor F_{model} is

$$F_{\text{MX}} = \left(\frac{3}{5}\right)^2 I_{\text{ivt}}(\kappa, 1, 1, 1) \qquad (39)$$

for the meson-exchange (MX) model, and is

$$F_{\text{XQQ}} = \left(\frac{8}{9}\right)\left(\frac{9\beta^{*2}}{5\beta^{*2} + 6b^2}\right)^{3/4} I_{\text{XQQ}}(\kappa, D_1, D_2, D_3) \qquad (40)$$
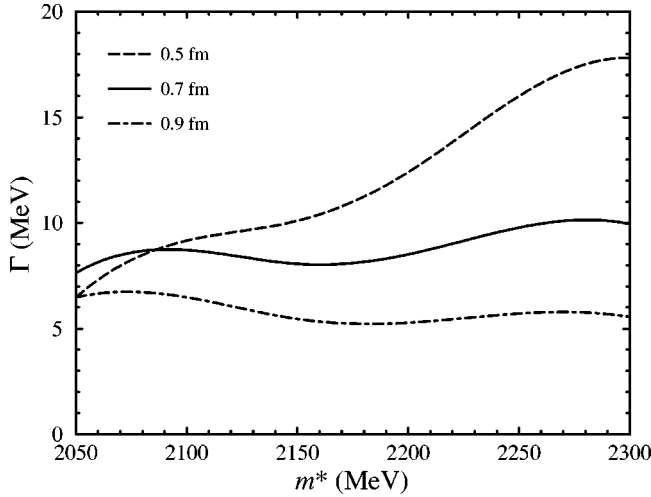
for the exchange-qq (XQQ) model. Here

FIG. 7. Decay width for $d^* \to NN$ as a function of the d^* masss m^* for different d^* wave function radii r^* using the Love-Franey t matrix at the final-state energy.

FIG. 8. Decay width for $d^* \to NN$ as a function of the d^* masss m^* for $r^* = 0.7$ fm using the Full Born potential in the Born approximation. The result for the Love-Franey t-matrix is also shown as a solid curve.

$$I_{\text{model}}(\kappa, D_1, D_2, D_3) = e^{-D_1 \kappa^2/2} \int e^{-D_2 Q^2/2} [j_2(iD_3 \kappa Q)$$

$$\times (\kappa Q)^3] t_{\text{model}}(\beta^* Q) Q \, dQ, \quad (41)$$

$\kappa = k^*/\beta^*$ is the dimensionless nucleon momentum in the c.m. frame, and $Q = q/\beta^*$ is the dimensionless momentum transfer. The elastic baryon form factor at each quark vertex is already contained in the NN interaction t_{ivt} of Eq. (21). Furthermore, the t matrix contains NN rescattering contributions to all orders of the NN interaction.

For the XQQ model, for which t_{xqq} in this equation refers to the function $V_0/(\mu^2 + q^2)$ in Eq. (35), the exchange baryon form factor appears explicitly in F_{xqq}. The latter depends on the dimensionless parameters D_i which are functions of the baryon size parameters β^* and $b = 1/r_p$, where $r_p = 0.6$ fm is the proton radius. For $r^* = 0.7$ fm, they have the numerical values of

$$D_1 = 0.214; \quad D_2 = 0.398; \quad D_3 = 0.153. \quad (42)$$

V. RESULTS FOR THE PARTIAL DECAY WIDTH

The partial decay width for $d^* \to NN$ can now be calculated numerically for the empirical Love-Franey NN t matrix, the Full Born potential treated in the Born approximation, and the OGE qq interaction with Pauli exchange.

The empirical LF t matrix used is evaluated at the equivalent nucleon lab energy

$$T_{\text{lab}} = \frac{m^{*2}}{2m} - 2m \quad (43)$$

of the final NN state. The resulting decay widths Γ, obtained by interpolating from the values calculated at the three nearest energies tabulated by LF, are shown in Fig. 7 as functions of the d^* mass m^* for different d^* wave function radii r^*.
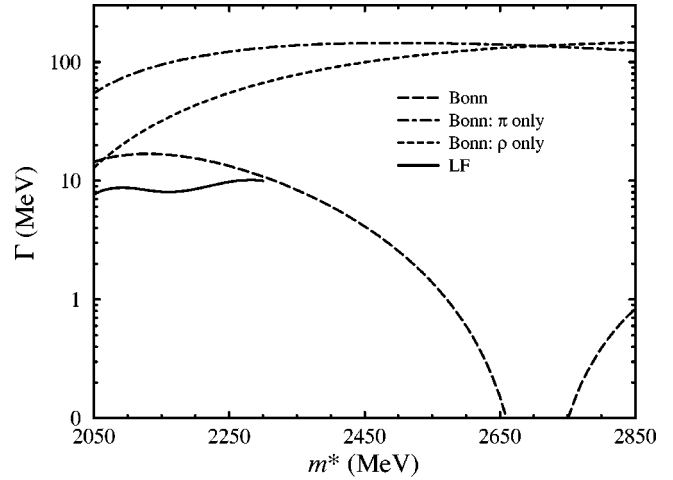
The dependence on these parameters is significant, but not strong, and is of a somewhat complex character.

The origin of some of the complexities in the behavior of Γ can be seen in Fig. 8, which gives the corresponding results for $r^* = 0.7$ fm covering a wider range of dibaryon mass calculated with the full Bonn potential treated in the Born approximation. The result is typically 2–3 times larger than those for the LF t-matrix in the mass range (2050–2130 MeV) of interest in the QDCS model, in qualitative agreement with the corresponding behavior in the production cross section. Note however that the leading decay process studied here is first-order in the interaction, but the leading production process is second order.

The ''π only'' contribution (shown as a dash-dot curve) is again much larger, here by another factor of three in this mass range. Even the ''ρ only'' result (given by the short dashed curve) is large, becoming in fact larger than even the ''π only'' contribution after 2690 MeV. This behavior is consistent with the fact that the decay involves interactions at shorter distances and higher energies than the production at TRIUMF energies. This means that the results for Γ is particularly sensitive to the cancellation between the π and ρ exchange interactions in our simple leading-order model. In fact, the vanishing of the calculated decay width due to the complete destructive interference between the π and ρ contributions can be seen in the figure at 2690 MeV.

For the XQQ interaction appropriate to the perturbative vacuum of the baryon interior, we find a result of $\Gamma = 77$ eV at $r^* = 0.7$ fm, $m^* = 2100$ MeV and a gluon mass of $\mu = 300$ MeV [41] if V_{xqq} interaction of Eq. (35) is treated as a direct qq interaction. (This is done by dropping the space-exchange operator $\mathcal{P}^x$ and adding baryon elastic form factors to the expression for Γ.) Because the qq interaction strength is always chosen to fit the $\Delta - N$ mass difference, the result is very insensitive to the choice of the gluon mass, being 71 eV if $\mu = 500$ MeV. Compared to the result of 22 MeV for ''ρ only,'' these are smaller by a factor of 3×10^5, in good agreement with the estimate based on the interaction strengths.

On restoring the space-exchange operator $\mathcal{P}^x$, we find that the width drops drastically by another factor of 3×10^6 to only 2.1×10^{-5} eV. The result is very sensitive to r^*, being 250 times larger for the smaller d^* radius of $r^* = 0.5$ fm. One reason why the result is so small is that the orbital angular momentum in the relative baryon-baryon coordinate is $L = 2$, where the centrifugal potential inhibits the quark exchange. If we had used $L = 0$ instead, the result would have been 2.3×10^{-3} eV, as compared to an $L = 0$ width of 190 eV when $\mathcal{P}^x$ is purposely dropped. We conclude from this that in the absence of stronger short-range components in both initial and final wave functions, quark-exchange effects are negligible.

Up to this point, we have done the calculation as if the interaction were 100% by meson exchanges via the meson cloud in the baryon exterior, or 100% by gluon exchange in the perturbative vacuum of the baryon interior. In reality, there is always some "external" contribution even when all the six quarks of d^* are in the same cluster. Since the external contribution is so much greater than the internal contribution, some of it will always survive to give a nonnegligible decay width. In the absence of a detailed model describing the precise proportion between the two contributions, we shall discount our calculated meson-exchange contribution by 50% as a guess of what a more realistic width should be.

The interior correction for gluon exchange discussed here does not apply to the lowest-order production calculated in Sec. III: The two mesons whose exchanges between projectile and target nucleons are responsible for the inelastic production of d^* are both external virtual mesons.

Is the meson-exchange interaction used here too strong? This can be answered partially by using the same method to calculate the decay width of that archtypical baryon decay $\Delta \to \pi N$. Using the πNN coupling constant of $f^2_{\pi NN}/4\pi = 0.078$ given by the full Bonn potential and reducing to a πqq coupling constant, we find a result of only 70 MeV, much less than the experimental value of 120 MeV. This result is in agreement with past calculations of this width [35]. One might be tempted to increase the calculated result by a factor of $(120/70)^2 \approx 3$, but this is not advisable because a real π on the energy shell is emitted in the Δ decay, whereas the $d^* \to NN$ decay involves virtual mesons off the energy shell [42]. The off-shell coupling constants that appear are more appropriately determined from nuclear forces, at least in principle. If we had been calculating the $d^* \to \pi NN$ decay by the same method, we would be justified to increase the calculated result by a factor $120/70 \approx 1.7$ for that vertex emitting the real pion.

VI. DEPENDENCE ON QUARK MODELS

The calculated d^* production cross section and decay width can be expected to depend sensitively on the quark wave function of the d^*, perhaps even more so than its theoretical mass. We shall consider qualitatively some of the issues involved.

One of these issues is the possibility of quark delocalization, which refers to the idea that under certain circumstances a quark may find it energetically favorable to be partly on the left side and partly on the right side of a dibaryon. The QDCS model [24] actually describes each quark in the d^*

wave function as 50/50 left or right. The six-quark d^* wave function then has the structure

$$
\begin{aligned}
(L+R)^6 = & L^6 + 6L^5R + 15L^4R^2 + 20L^3R^3 \\
& + 15L^2R^4 + 6LR^5 + R^6 \\
\to & 2(L^6 \text{ or } R^6) + 12(L^5R \text{ or } LR^5) \\
& + 30(L^4R^2 \text{ or } L^2R^4) + 20(L^3R^3). \quad (44)
\end{aligned}
$$

After the projection of relative S-states between the clusters and a correction for the position of the center of mass, the wave function simplifies to the form shown after the right arrow. Its components fall roughly into two groups: There is a group of normal ("n") clusters of q^{3m} configurations made up of L^3R^3, L^6 and R^6 with no delocalized quark. They have the probability of

$$
P_n = (2^2 + 20^2)/1448 \approx 0.28. \quad (45)
$$

The remaining group of components L^5R, LR^5, L^4R^2, and L^2R^4 has one delocalized quark ("dq") away from a normal q^{3m} configuration, and the remaining probability of $P_{dq} = 1 - P_n \approx 0.72$.

For the normal group, the projection of S states makes the wave function spherical symmetric in the relative baryon-baryon coordinate, and very similar to the Gaussian wave function of our didelta model. In fact, the maximum overlap between the two wave functions is close to 100%. There is to be sure some depression of the two-center relative wave function near the origin of the relative coordinate, but the effect is quite unimportant in the wave function overlap. The behavior of the short-distance wave function is probably much more important in the production and decay processes considered in this paper, but it is likely that the short-distance wavefunction is not very good in both models. Furthermore, the q^6 component is entirely absent in the didelta model and is probably too weak in the QDCS model.

Though subject to these additional uncertainties, our counting suggests that this normal group will contribute essentially the full amount, i.e., about 28% of that calculated in our model in both decay and production.

For the abnormal components with one "wrong-way" quark, the contribution could be very different, especially if there is special coherence between the normal and abnormal amplitudes. We are not in a position to estimate such coherent contributions because it would require a specific model. As far as its incoherent contribution is concerned, the worse that can happen is that it will vanish. This must be a rather extreme situation, because three of the nine pairs of interacting quarks involve the "wrong-way" quark, and the interaction could scatter it back to form a normal cluster structure. In the remaining six pairs, the "wrong-way" quark is a spectator, which requires a wave function overlap to get back to normal. There is thus a reduction in the calculated decay or production amplitude of the order of 1/2 or $1/e$ for the spectator contribution, more if the clusters are farther apart. We

then end up with an estimate for the decay width or production cross section of the order of 7–20 % from these abnormal components.

Thus very crudely, we expect the delocalization to reduce the calculated decay width or production cross section by a factor of 1/2–1/3.

Another model-dependent issue is the contribution of hidden-color (HC) configurations. Our didelta model used without quark exchanges between the two baryon clusters contains no HC component. In contrast, most quark models of the d^* contains 80% HC components where the first three quarks are in a color-octet state. These HC components are expected to contribute less, perhaps significantly less, than the baryon-baryon components. A calculation of their contributions using the method of this paper is now underway. For the time being, we shall allow for some contributions from the HC components by reducing the baryon-baryon results by a factor of 1/2. (The reduction factor is 1/5 when the HC components contribute nothing.)

The final educated guesses for d^* decay and production for the quark-delocalization model used with the Love-Franey NN t matrix at $m^*=2.1$ GeV and $r^*=0.7$ fm are as follows: The decay width is decreased from 9 MeV to about 1 MeV when an "interior" correction of 1/2 and an octet-octet reduction factor of 1/2 are also included. The production cross section at TRIUMF energy is reduced from 13 to about 2 μb/sr at the second maximum.

VII. DISCUSSIONS AND CONCLUSIONS

The leading-order processes studied here suggest that the inelastic production cross section of d^* might be in the μb/sr range, while its decay width into two nucleons might be in MeV's. Love-Franey empirical NN t-matrices are used to include all NN rescattering effects to all orders in the decay and in an impulse approximation for the production. Other aspects of the reported calculations are not sufficiently realistic because of approximations made in the hadron wave functions and in the treatment of the reaction mechanisms. It is worthwhile to enumerate the most serious of these problems.

The Glauber multiple-diffraction model used in the calculation of the production cross section might be quite good for elastic scattering at small angles. Its validity for large inelasticities and at large angles is unknown. It is necessary to correct for effects neglected by the Glauber model, especially at large angles [43]. However, there is probably no point in doing this unless one can also include higher-order production processes. These are the usual difficulties connected with the calculation of strong-interaction cross sections, and as usual, we see no simple solution.

The baryon models used for both d and d^* are very crude. The S-state wave function used for the deuteron target tends to underestimate the high-momentum components of the target baryons. To be more realistic, one should include the D-state of the deuteron, and probably also the D-state of d^*. Since d^* production depends so much on these high-momentum components, one could argue that the present S-state results give conservative lower bounds on the production cross section.

Depending on the model, we need to add other short-

distance refinements such as delocalization and hidden-color states to these wave functions. The inclusion of these features are not intrinsically difficult, although they can be tedious to execute. The difficulty lies instead in the lack of knowledge on how strong these components are. Studies of the effects of short-distance wave functions require sustained efforts.

In the calculation of the partial $d^*\rightarrow NN$ decay width, it is necessary to account more carefully for the role played by external meson exchanges versus internal gluon exchanges. It is obvious that this too cannot be done on a quantitative basis without a more realistic model of the d^* wave function. It will be necessary to include higher-order processes not yet included by using NN t matrices.

In addition, the decay width could be dominated by the $(\pi)^n NN$ branches for sufficiently large d^* mass. It is necessary to understand these partial decay widths at least qualitatively.

The theoretical picture concerning the dibaryon d^* at the present time seems to be as follows: Its calculated mass has been in the range 2050 [24] –2840 [8] MeV. Its inelastic production cross section could be significant, i.e., in the μb/sr range. Its partial decay width into two nucleons is probably in MeV's for the low-mass candidate. Because its calculated mass is so sensitive to certain assumptions concerning quark dynamics in hadrons, any positive or negative experimental information on its presence in a certain mass range has interesting implications.

What is the experimental situation concerning isoscalar dibaryons? A dibaryon search was made at Saturne by measuring the spectra for missing masses between 1.9 and 2.35 GeV using the $dd\rightarrow dX$ reaction for 2.29, 2.00, and 1.65 GeV deuteron beams. An upper limit of 30 nb/GeV^2 was found for the invariant production cross section of a dibaryon if its width is less than several tens of MeV [4]. This result is for the missing mass of 2.16 GeV and for a 2.00 GeV deuteron beam with deuterons detected at 27° (lab), or 69.3° (c.m.). It corresponds to a c.m. differential production cross section at this angle of only 15 nb/sr in the dd reaction. It is not easy to extract a pd bound from this result partly because of the presence of an elastic form factor for the intact deuteron [44], which causes a large reduction in the dd production amplitudes relative to the pd amplitude for production from single nucleons in the intact deuteron. An additional complication is that for the dd reaction, the d^* can also be produced by another double-scattering process that involves both nucleons of the intact d. Its contribution can be expected to be similar in structure, but probably reduced in value, when compared to that of production from a single nucleon in the pd reaction. This process must also be included in the interpretation of dd cross sections. This means that any extraction of a pd bound from the dd bound will depend on a model-dependent theoretical analysis, and cannot be a pure experimental bound.

To my best knowledge, the only direct experimental upper bound for resonance production in the pd reaction is an unpublished LAMPF experiment based on the $d(\vec{p},p)X^+$ reaction at $T_p=798$ MeV and 15.1° (lab). The results are in the range of 1–4 μb/sr/MeV [5] dependent on the missing mass in the missing-mass range of 1865–2200 MeV. They

are of the same order as the very rough theoretical estimates of d* production given in this paper. Hence no definite conclusion can be drawn from a comparison between them.

It thus appears that the present theoretical picture is still very unrealistic and incomplete. Much additional work is needed, especially on the partial decay widths in pionic channels for which there is at present very little quantitative information. However, the question of dibaryons is ultimately an experimental question. A new dibaryon search with a sensitivity much greater than the known LAMPF bound will be needed to advance our understanding of the situation.

[1] R. L. Jaffe, Phys. Rev. Lett. **38**, 195 (1977).

[2] P. J. G. Mulders, A. T. M. Aerts, and J. J. de Swat, Phys. Rev. D **17**, 260 (1978).

[3] LISS (Light Ion Spin Synchrotron) White Paper, January, 1995, Indiana University Cyclotron Facility at http://www.iucf.indiana.edu/Publications/LISS.html

[4] M. P. Combes *et al.*, Nucl. Phys. **A431**, 703 (1984).

[5] K. K. Seth, B. Parker, C. M. Ginsburg, and R. Soundranayagam, contributed paper to PANIC-90 Particles and Nuclei Conference, Boston, 1990 (unpublished).

[6] I. P. Auer *et al.*, Phys. Rev. D **34**, 2581 (1986).

[7] J. Ball *et al.*, Phys. Lett. B **320**, 206 (1994).

[8] P. Gonzalez, P. LaFrance, and E. L. Lomon, Phys. Rev. D **35**, 2143 (1987).

[9] A. W. Thomas, S. Théberge, and G. A. Miller, Phys. Rev. D **24**, 216 (1981).

[10] E. L. Lomon, in Proc. Workshop on future directions in particle and nuclear physics at multi-GeV hadron beam facilities, BNL-52389 (BNL, 1993), pp. 406–411.

[11] P. J. G. Mulders and A. W. Thomas, J. Phys. G **9**, 1159 (1983); K. Saito, Prog. Theor. Phys. **72**, 674 (1984).

[12] C. W. Wong, Prog. Part. Nucl. Phys. **8**, 223 (1982).

[13] I. P. Auer *et al.*, Phys. Rev. Lett. **62**, 2649 (1989).

[14] B. P. Adiasevich *et al.*, Z. Phys. C **71**, 65 (1996).

[15] E. L. Lomon, unpublished 1997 report, nucl-th/9710006 (MIT-CTP-2680).

[16] R. Bilger *et al.*, Z. Phys. A **343**, 491 (1992); R. Bilger, H. A. Clement, and M. G. Schepkin, Phys. Rev. Lett. **71**, 42 (1993); **72**, 2972 (1994).

[17] L. S. Vorobev *et al.*, JETP Lett. **59**, 77 (1994).

[18] W. Brodowski *et al.*, Z. Phys. A **355**, 5 (1996).

[19] M. A. Kagarlis and M. B. Johnson, Phys. Rev. Lett. **73**, 38 (1994).

[20] P. J. Mulders, A. T. Aerts, and J. J. de Swart, Phys. Rev. D **21**, 2653 (1980).

[21] L. A. Kondratyuk, B. V. Artemyanov, and M. G. Schepkin, Sov. J. Nucl. Phys. **45**, 776 (1987).

[22] G. Wagner, L. Ya. Glozman, A. J. Buchmann, and A. Faessler, Nucl. Phys. **A594**, 263 (1995).

[23] E. L. Lomon, J. Phys. (Paris), Colloq. **58**, C6-363 (1990).

[24] T. Goldman, K. Maltman, G. T. Stephenson, Jr., K. E. Schmidt, and F. Wang, Phys. Rev. C **39**, 1889 (1989); F. Wang, J. L. Ping, G. H. Wu, L. J. Teng, and T. Goldman, *ibid.* **51**, 3411 (1995).

[25] F. Wang, G. H. Wu, L. J. Teng, and T. Goldman, Phys. Rev. Lett. **69**, 2901 (1992).

[26] T. Goldman, K. Maltman, G. T. Stephenson, Jr., J. L. Ping, and F. Wang, ''Systematic Theoretical Search for Dibaryons in a Relativistic Model,'' Los Alamos Report LA-UR-95-2609.

[27] K. Johnson, Acta Phys. Pol. B **6**, 865 (1975).

[28] T. A. DeGrand, R. L. Jaffe, K. Johnson, and J. Kiskis, Phys. Rev. D **12**, 2060 (1975).

[29] Yu. S. Kalashnikova, I. M. Narodetskii, and Yu. A. Simonov, Yad. Fiz **46**, 1181 (1987) [Sov. J. Nucl. Phys. **46**, 689 (1987)].

[30] M. Gonin, Nucl. Phys. **A610** [NA50], 404c (1996); C. Lourenco, *ibid.* **A610** [NA50], 552c (1996).

[31] J.-P. Blaizot and J.-Y. Ollitrault, Phys. Rev. Lett. **77**, 1703 (1996).

[32] T. Matsui and H. Satz, Phys. Lett. B **178**, 416 (1986).

[33] R. Machleidt, K. Holinde, and Ch. Elster, Phys. Rep. **149**, 1 (1987); R. Machleidt, Adv. Nucl. Phys. **19**, 189 (1989).

[34] R. J. Glauber, in *High Energy Physics and Nuclear Structure*, edited by S. Devons (Plenum, New York, 1970), p. 207.

[35] G. E. Brown and W. Weise, Phys. Rep., Phys. Lett. **22C**, 279 (1975).

[36] M. A. Franey and W. G. Love, Phys. Rev. C **31**, 488 (1985).

[37] J. A. Wheeler, Phys. Rev. **52**, 1083 (1937); **52**, 1107 (1937).

[38] N. K. Glendenning, *Direct Nuclear Reactions* (Academic Press, New York, 1983), pp. 194 and 195.

[39] M. Harvey, Nucl. Phys. **A352**, 301 (1981).

[40] J. J Sakurai, *Advanced Quantum Mechanics* (Addison-Wesley, Reading, MA, 1967), pp. 171–172.

[41] C. W. Wong, Phys. Rev. D **54**, R4199 (1996).

[42] H. Sugawara and F. von Hippel, Phys. Rev. **185**, 2046 (1969).

[43] C. W. Wong and S. K. Young, Phys. Rev. C **12**, 1301 (1975); S. K. Young and C. W. Wong, *ibid.* **15**, 2146 (1977).

[44] S. Yen (private communication).